Application Note 61
femtoFBG

A versatile machine optimized for the fabrication of Fiber Bragg Gratings (FBGs) by femtosecond laser direct-writing

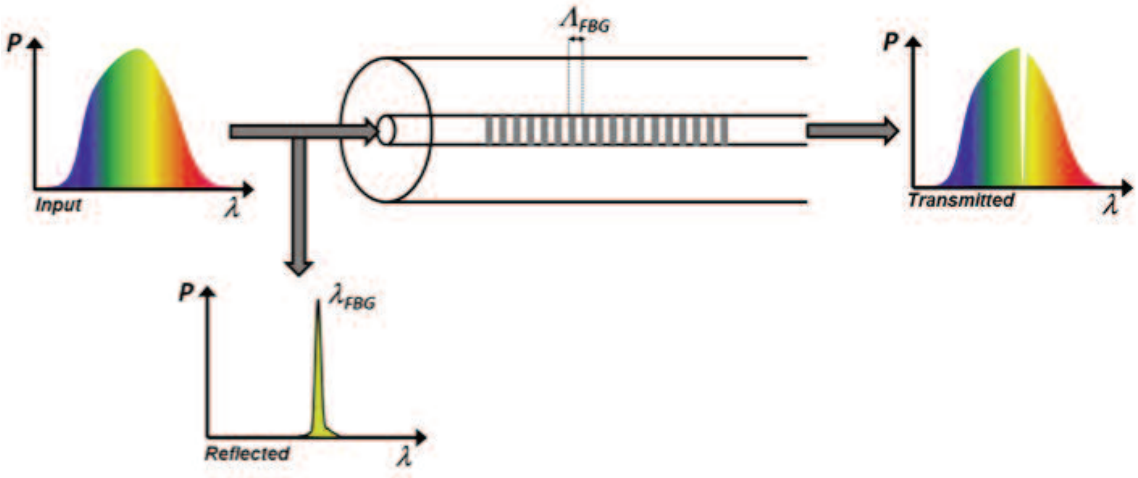

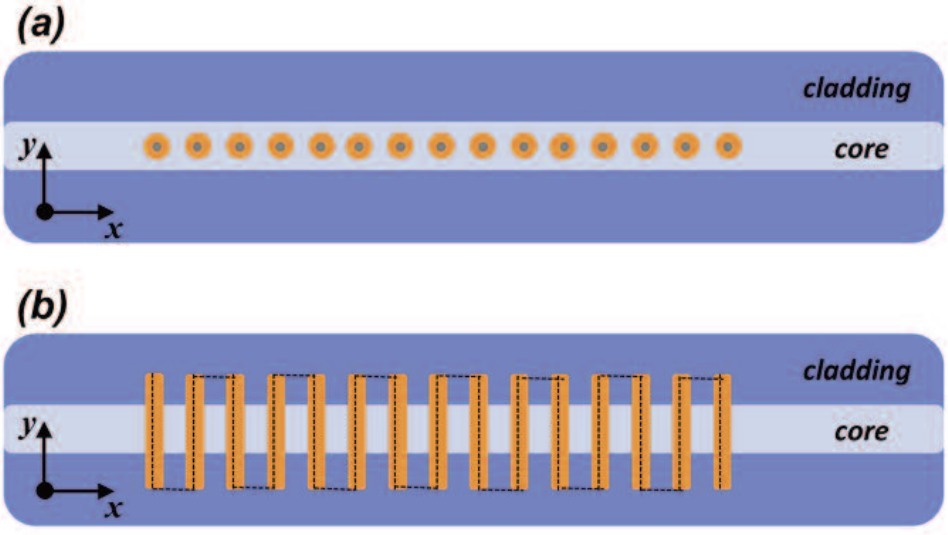

Newport is proud to release the first commercially available workstation for fiber Bragg grating manufacturing based on femtosecond laser direct-writing, the *femto*FBG. This is the ideal tool for the end-user interested in combining fabrication speed and accuracy with Bragg grating design flexibility. The femtoFBG is capable of writing Bragg gratings in a large variety of fibers, from diverse materials to exotic structure designs making it an enabling tool for a multitude of R&D applications.

Introduction

Fiber Bragg gratings (FBGs) are common components in modern optical communication networks. They are also used in dispersion compensation and wavelength selective devices, fiber lasers, band-rejection filters, and fiber taps, just to name a few [1]. Furthermore, FBGs are extensively employed for sensing strain and temperature changes in industries such as mining, aircraft manufacturing, structural civil engineering and power transmission lines [2]. The wide-spread use of FBGs as sensors stems from their ability to perform read-out tasks in harsh environments. They possess several qualities that make them more attractive than metal strain gauge counterparts. FBGs can measure strains larger than 10,000 μm/m, are immune to electromagnetic interference, are not distance dependent, are intrinsically passive, and are small in size and light-weight allowing for ease of installation with minimal intrusion [3].

The most common way to fabricate FBGs is by means of interference lithography, using a UV laser to imprint a periodic pattern within the core of a fiber [4]. The sensitivity of the core to the excitation source is typically augmented by chemical doping and/or a process of hydrogen loading. Traditionally, the UV fringe pattern necessary to create an FBG is generated using either a Lloyd or a prism interferometry scheme, or by splitting the UV laser beam in two paths and recombining them on the sample at specific angles. It is now common to use a phase mask, which has a simpler optical path. When the excitation beam interacts with the phase mask, a near-field image is created by the interference of the plus and minus first-order diffracted beams. The desired FBG is created by positioning the fiber in the plane of this interference pattern.

These fabrication methods are clearly attractive from a production point of view since they allow for rapid and reliable manufacturing. Nonetheless, they lack a series of characteristics that renders them too rigid for R&D applications where fast, flexible prototyping is essential. For example, the fiber must be stripped of its polymer coating prior to UV (< 250 nm) irradiation, rendering it susceptible to fractures and forcing a re-coating step after the formation of the grating. Optimal results are obtained only when photosensitive fibers are used. Besides being more expensive, the modification of the refractive index in these fibers is reversible making their use at high temperature limited. Perhaps more importantly, interferometric methods are limited in the type of FBG that can be fabricated. For example, a specific phase mask is required for each combination of FBG Bragg wavelength and pattern geometry desired. Finally, the strength of FBGs manufactured by interferometric methods display an undesirable thermal decay at high temperatures.

An alternative method to the fabrication of an FBG is the use of a femtosecond laser direct-write process [5]. In this case, the fiber core refractive index pattern can be modified permanently and the properties of the written pattern can be custom-tailored with great freedom. Compared to traditional methods, FBG writing by femtosecond lasers can be applied successfully to a wide variety of fibers from standard ones used in telecommunications to sapphire fibers used in high temperature environments. Additionally, writing of FBGs with femtosecond lasers can done without removing and subsequently replacing the fiber polymer coating, since the materials typically used (acrylate and polyimide) are transparent to the near-infrared region of the spectrum.

In this application note, we describe Newport's *femtoFBG* (Figure 1), a specially designed workstation for femtosecond laser direct-writing of FBGs. When used in conjunction with Spectra-Physics' Spirit laser, the *femtoFBG* offers end-users the speed and flexibility required in R&D applications. After detailing the *femtoFBG* system architecture, we present several examples of FBG manufacturing that highlight the *femtoFBG* operation and capabilities.

Figure 1 – *FemtoFBG, femtosecond laser direct-write workstation for the manufacturing of fiber Bragg gratings.*

Definitions

In an FBG, the refractive index of the core is periodically modulated along the fiber's main axis (Figure 2). The period of the modulation ranges typically from a few hundred nanometers to a few microns. When light is launched into an FBG, it experiences a certain amount of scattering at each grating

plane. Most of the scattered light becomes more and more out-of-phase and eventually decays due to deconstructive interference. If the Bragg condition is satisfied for one of the colors of the input light, then a sharp reflected peak is observed in the backward direction with a center wavelength determined by the grating's parameters. The FBG is in essence a device capable of reflecting light of a specific wavelength, i.e. a band-rejection optical filter [6}

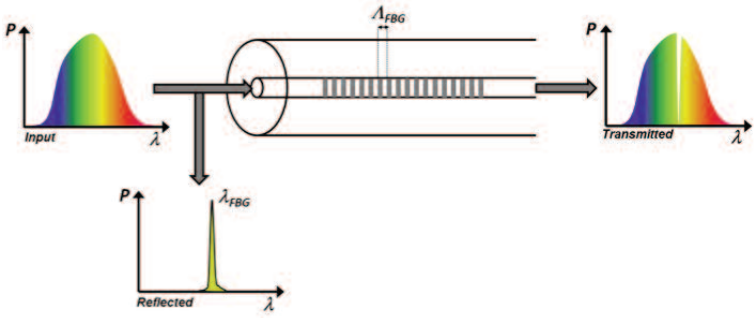

Figure 2 – Schematic of a fiber Bragg grating and representative transmission and reflection spectra.

In order to satisfy the Bragg condition, the reflected light in an FBG must fulfill both energy and momentum conservation. From an energy point of view, the requirement is that the frequency of the incident radiation equals the frequency of the reflected radiation ($\hbar\omega_i = \hbar\omega_f$). Momentum conservation requires that the wave vector of the reflected radiation totals the sum of the incident and grating wave vectors (kf = ki + K). Considering that the magnitude of the incident wave vector is identical to that of the reflected wave vector, but opposite in sign, and that the grating wave vector has a magnitude of $2\pi/\Lambda_{FBG}$ (Λ_{FBG} is the period of the refractive index modulation), the momentum conservation yields the Bragg condition. For a general m-order

$$\lambda_{FBG} = \frac{2n\Lambda_{FBG}}{m} \quad (1)$$

process, it becomes where λ_{FBG} is the wavelength of the input light that is reflected by the grating and n is the effective refractive index of the fiber core at the reflection wavelength. Using equation 1, it can be seen that a 1st order FBG operating at telecommunications wavelengths needs to have a grating with a period only a few hundred nanometers wide. Considering that the length of FBGs is ordinarily more than a few millimeters long, it follows that the method for fabricating these optical devices must possess extraordinary precision and accuracy.

In many applications, it is important to use FBGs that produce strong reflective bands with narrow widths (< 0.5 nm). To understand how experimental conditions can influence the properties of FBGs' reflection bands, it is important to introduce the coupling coefficient (κ) defined as $(\pi/\lambda_{FBG})\cdot\Delta n$ where Δn is the refractive index perturbation in the fiber core [7]. For an FBG with a small Δn and a constant grating period, the reflectivity and bandwidth of the rejected mode are where L is grating length.

$$R = tanh^2(\kappa L) \quad (2)$$

$$\Delta\lambda = \frac{\lambda_{FBG}^2}{2n}\cdot\frac{1}{L}\sqrt{\left(\kappa L/\pi\right)^2 + 1} \quad (3)$$

It is evident that the bandwidth of an FBG reflection band depends both on the grating coupling coefficient and length. A closer examination of equations 2 and 3 shows that under certain conditions one parameter will have a stronger influence over the other one. For example, at reflectivities less than 60% (κL < 1), the FBG bandwidth scales proportionally with the inverse of the grating length. Thus, a longer grating will produce a narrower reflection band. However, when reflectivities reach values higher than 99% (κL >10), FBG bandwidths become linearly dependent with κ. In this case, narrower bandwidths are accomplished by reducing Δn or increasing the order m of the grating.

FBGs use as sensors, resides in the relationship described in equation 1. The center wavelength of the reflected band depends on the grating period and the effective refractive index of the core. Both parameters can be affected by externally applied mechanical and thermal perturbations [8]. For example, under an applied strain ε along the fiber main axis, the period of the grating is changed by compression or expansion producing a shift Δλ in the Bragg wavelength. This effect is proportional to $(1 - p_e)\cdot\varepsilon$ where p_e is the material strain-optic constant ($0.22\cdot10\text{-}6\ \mu\varepsilon^{-1}$ for silica). Typical sensitivity to an applied axial strain is around 1nm/millistrain. The influence of temperature is more complex, since it can change both the material refractive index and the grating spacing due to thermal expansion. Thus, the Bragg wavelength shift due to a temperature variation of ΔT is proportional to $(\xi + \alpha)\cdot\Delta T$ where ξ is the material thermo-optic coefficient and α is the material thermal expansion coefficient. Since in silica ξ and α are $8.6\cdot10\text{-}6\ °C^{-1}$ and $0.55\cdot10\text{-}6\ °C^{-1}$, respectively, the thermal effect on the refractive index is the predominant process that renders standard FBGs sensitive to environmental temperature changes. In this case the sensitivity is around 10 pm/°C.

Manufacturing Procedures

There are two methods to create FBGs by femtosecond laser direct-writing. In one, each grating plane is formed by either a single laser shot or by a multitude of laser shots in a point-by-point (PbP) fashion [9,10]. In the other, line-by-line (LbL), a series of parallel lines are written perpendicularly to the fiber main axis covering a distance defined by the length of the Bragg grating [11]. In both cases, the space between the points or the lines, as well as the magnitude of the refractive index modulation are determined by the user based on the desired application. A schematic representation of the results of the two aforementioned writing strategies is shown in Figure 3 where the fiber main axis is arbitrarily chosen to be the x axis. In this picture, cross-sections of the grating patterns formed by PbP and LbL writings are shown; in particular, a top-view was chosen where the plane of the paper is perpendicular to the direction of the laser

used for grating inscription (z axis). While the PbP writing volume is confined entirely within the core of the fiber, LbL writing extends beyond the core and into the cladding.

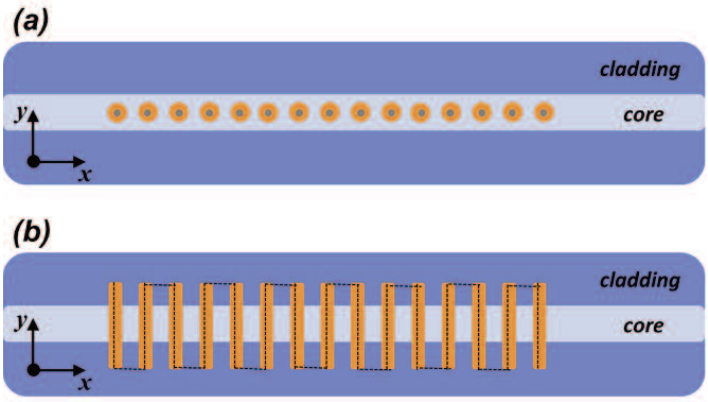

Figure 3 – Results of different writing methodologies for producing FBGs. In PbP (a), refractive index modulation is confined within the fiber core and it results from the interaction with the fiber of either single or multiple laser pulses per spot. In LbL (b), the periodic pattern of high and low refractive indices is formed by writing a series of parallel lines perpendicular to the fiber main axis. The areas in orange represent locations in the fiber that were treated with the femtosecond laser. The black dotted lines and circles delineate the laser writing patterns. While a point-by-point method is used in (a), a symmetric raster scan is employed in (b). Both images in (a) and (b) represent cross-sections of laser written FBGs where the plane of the paper (xy) is perpendicular to the direction of the laser (z).

A common way to write FBGs with the PbP method is to use each laser pulse to create a grating plane [12]. To accomplish this, the fiber is moved along its main axis at a speed vtrans so that the grating period Λ_{FBG} is now defined by the ratio vtrans/fr

$$\lambda_{FBG} = \frac{2nv_{trans}}{mf_r} \quad (4)$$

where fr is the laser repetition rate. Thus, equation 1 for an FBG written in a PbP manner becomes equation 4.

This method of writing FBGs is not only rapid (typical translational stage speeds are on the order of millimeters per second), but it provides great design flexibility. For example, changing the speed of the stage creates Bragg effects at different wavelengths. Furthermore, chirped gratings can easily be manufactured by varying the translational speed during the writing process [13].

Instead of using a single laser pulse per grating plane, the PbP method can be used also with a burst of laser pulses. In this case, either a mechanical or an opto-mechanical shutter is used to precisely control the laser exposure time so to have exactly the same number of pulses per grating plane. The process is then carried on through a move-stop irradiation scheme that is repeated for the entire length of the grating.

In LbL writing, the fiber is translated by two high-resolution stages following a symmetric raster scan pathway. The grating period (Λ_{FBG}) is defined by the spacing between the lines in the raster scan (Figure 3b). The laser exposure is synchronized with the stages motion to ensure laser exposure only along the vertical lines (y direction) of the raster scan.

In both methods described so far, femtosecond laser direct-writing of FBGs requires the movement of the optical fiber underneath a fixed and focused laser beam. In order to create a strong and efficient Bragg effect, the spacing between the grating planes needs to be reproduced with high precision for a long distance. Moreover, the writing within the fiber needs to be consistent at the same location in z along the entire grating. This is not trivial and requires high-end hardware and special precautions. The scientists and engineers in the Technology and Applications Center at Newport Corporation have established a *femtoFBG* alignment protocol that offers accurate and repeatable FBG manufacturing.

Although a complete understanding of the mechanism creating the refractive index modulation in optical fiber when using femtosecond laser direct-writing is still lacking, a classification based on the characteristics of the material modification has being widely accepted [14,15]. When a femtosecond laser with low pulse energy is focused onto a fiber, a combination of multiphoton absorption and photoionization occurs simultaneously that leads to localized melting of the glass followed by resolidification.

During this process, a rapid change of the glass state from solid to liquid and then back to solid takes place. It is this phenomenon that causes the formation of the change of the material refractive index in FBGs. The alteration of the fiber based on these mechanisms is termed Type I-IR where IR refers to the wavelength of the laser used during the writing. It is important to specify the laser wavelength since, for example, Type I-UV gratings are formed without glass melting.

When a femtosecond laser with high pulse energy is used, the affected area of the fiber presents a void surrounded by a high density glass shell. In this case, the ultimate result is caused by avalanche ionization that leads to a localized plasma formation. When the charge density is high enough, a Coulombic explosion takes place that pushes material outwards. FBGs formed through this type of modification are termed Type II-IR.

FBGs fabricated by femtosecond laser direct-writing enjoy several advantages versus traditional methods used for creating commercially available FBGs (interference lithography using nanosecond pulsed UV lasers).

First, refractive index change caused by femtosecond lasers irradiation is three to four times larger than that caused by UV lasers ($6 \cdot 10^{-3}$ vs $2 \cdot 10^{-3}$). Second, photosensitive fibers are not needed anymore. Material choice flexibility when using femtosecond lasers allows for inclusion of photonic crystal fibers, sapphire fibers, and double-clad Yb-doped fibers. Also, writing Bragg grating in fibers using femtosecond lasers does not require the stripping of the polymer coating. One advantageous aspect of using interference lithography versus direct writing is the amount of optical coupling into cladding modes. While the index modulation follows a sinusoidal wave pattern in the core of FBGs created by interference lithography with a UV laser, the index modulation approximates a more square wave in a femtosecond direct-written FBG. The discontinuous modulation of the refractive index in femtosecond laser direct-written FBGs causes the formation of forward propagating coupling modes in the fiber cladding.

There are two intrinsic properties of FBGs fabricated by femtosecond laser direct-writing that make them unique [16]. One is the high thermal stability. For example, a Type II-IR grating was characterized with no noticeable change in the FBG reflectivity at temperatures up to 900° C. This is in contrast to FBGs fabricated in photosensitive glasses where the refractive index modulation is erased at 700° C. The other property is birefringence. The focusing geometry used in the laser direct-writing results in a local refractive index modification that is elongated in one direction creating polarization dependence. FBGs manufactured by femtosecond laser direct-writing exhibit different grating strengths for orthogonal input polarizations.

femtoFBG – Hardware

The *femtoFBG* (Figure 4) is designed specifically for manufacturing FBGs by femtosecond laser direct-writing with Spectra-Physics' Spirit laser. The femtoFBG gives the user great flexibility in the design of FBGs and the writing parameters used to produce them.

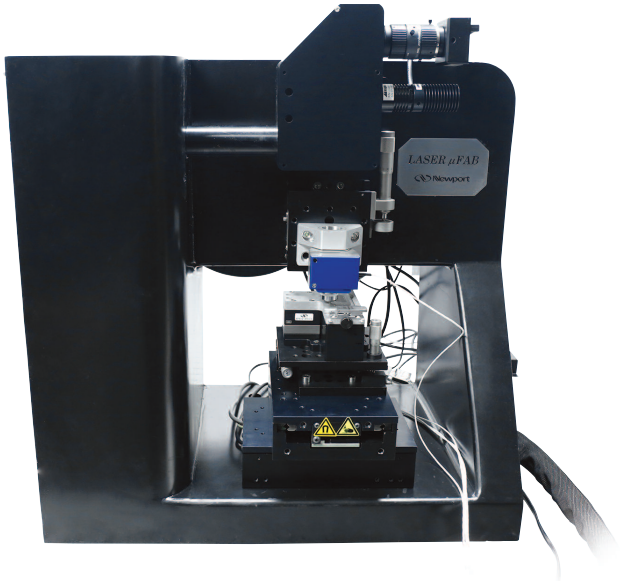

Figure 4 – Front view and side view pictures of Newport's femtoFBG.

The framework of the femtoFBG is made from a single piece of granite composite, manufactured by mineral casting. Traditional laser machine tools are assembled using cast iron or solid machined granite pieces because of their thermal stability, flatness, and vibration damping. Mineral castings offer significant weight and thermal mass to provide excellent thermal and vibrational stability. Producing the *femtoFBG* framework using mineral casting technology creates a compact, but stable and functional design.

The laser beam entrance height into the *femtoFBG* matches the height of the Spirit laser output. After entering the *femtoFBG*, the laser beam is routed vertically through a series of conditioning optics prior to the imaging and writing units (figure 4b). In the conditioning section of the system, a pair of lenses is used to expand the laser beam diameter to better match the microscope objective back aperture (~ 9 mm). Furthermore, the laser average power is controlled by a computer-controlled variable beam attenuator and then sampled and monitored with a photodiode. A quarter-wave plate converts the polarization of the laser beam from linear to circular.

The writing and imaging sections of the *femtoFBG* are designed to operate similarly to an upright microscope, with the sample located under the microscope objective. A dichroic mirror reflects the laser beam through the microscope objective and focuses the light into the sample. The microscope objective employed in FBG writing is a 40x, plan-neofluar with a numerical aperture of 0.75. Above the dichroic mirror resides the imaging system. This is capable of performing both transmission and reflection light microscopy, enabling the user not only to carefully position and align the sample in the writing plane, but also to monitor the writing process in real time.

The coarse position of the laser focal plane in the z direction is controlled with a vertical manual stage that has a range of two inches, and fine position is controlled with a piezo collar stage that has nanometer resolution, accuracy, and repeatability within a total travel distance of 500 µm (Piezosystem Jena, MIPOS 500). The sample can be moved arbitrarily in the x and y directions with the help of two linear stages (Newport, XMS100) stacked one on top of the other. The XMS is a high performance stage with minimum incremental motion, repeatability, and accuracy of 1 nm, 50 nm, and 1.4 µm, respectively. These features hold true along the entire 100 mm travel range of the stage, allowing ultraprecise motion. A manual multi-axis tilt platform (Newport, M-37) is added to the XY stages stack, to provide tilt and rotation adjustments for fiber alignment purposes. Specifically, it provides full, three-axis angular freedom with two tilt and one rotation adjustments using Vernier micrometer with 1 µm reading. The M-37 is capable of orienting a component parallel to an arbitrary plane. Finally, a custom-designed sample holder is placed at the top of the XY and tip-tilt-rotation stages assembly. The sample holder has two bare fiber magnetic clamps with precision machined V-grooves (Newport, 561-FH). The two clamps hold the fiber straight and in tension, allowing a section of the fiber approximately 2.5 inches (63.5 mm) long to be laser processed. The same holder also contains the accessories required to perform transmission illumination.

Most of the published work in the field of FBG manufacturing relies on the use of air-bearing stages. Although retaining the highest degree of flatness, air-bearing stages add cost and complexity to any systems in which they are implemented. To avoid these aggravations, we designed the femtoFBG with Newport XMS stages without sacrificing system performance. By means of the *femtoFBG*, FBGs with excellent mechanical, thermal and optical properties can be manufactured.

The optics within the *femtoFBG* can be configured for the output of two types of femtosecond lasers. In one case, reflective and transmissive optical components capable of working at both 520 nm and 1040 nm and possessing high energy damage thresholds are used in order to accommodate the emission of a Spectra-Physics Spirit laser. In the other case, NIR optics with minimal group velocity dispersion are used with the output of a Spectra-Physics Spitfire or Solstice laser. The *femtoFBG* is delivered with a personal computer loaded with proprietary software developed by the engineers and scientists in the Technology and Applications Center at Newport Corporation. With this tool, the operator has full control of all experimental conditions from irradiation parameters to complex motion within an easy to use customer inspired GUI.

femtoFBG – Sample preparation and alignment

The fiber used in the examples shown in this application note is Corning single-mode fiber SMF-28. The sample preparation and alignment procedures described in this section can be extended to other type of fibers. SMF-28 is a step-index, all-glass fiber that supports light propagation at 1310 nm and 1550 nm. Because of the low attenuation and low bending losses, SMF-28 is employed in long-haul and fiber-to-the-home applications. Core and cladding diameters of SMF-28 are 8.2 µm and 125 µm, respectively. The fiber comes with a double acrylic polymer coating with a diameter of 245 µm. The cladding refractive index is 1.444 at 1.55 µm and the core-cladding difference is about 0.35%. The higher refractive index of the fiber core is due to 3% molar doping with Germanium.

The focused laser beam experiences several distortion effects when passing through the fiber. This is due to the geometry of the fiber that acts for all intents and purposes as a cylindrical lens [17]. Besides creating optical distortions on the imaging side, making the visualization of the sample difficult, the lensing effect of the fiber causes the laser beam to be more and more elongated as it moves toward the core. This reduces laser intensity and the sum of these changes creates a different modification in the fiber than expected. To greatly eliminate these distortion effects, the fiber is immersed in an index-matching gel (for instance, Cargille cat#24317) during laser processing. In this medium, the fiber is easy to image and its elements (core and cladding) can be discerned with confidence. Furthermore, the distortion of the focused laser beam becomes greatly diminished, making writing the desired pattern less sensitive to the laser beam location within the fiber.

The sample consists of non-stripped SMF-28 sandwiched between a microscope slide (for instance, Ted Pella 26008, 75 x 25 x 1 mm) and a cover-slip (for instance, Ted Pella 260360, No. 1, 24 x 60 mm). The space between the two glasses is filled with the index-matching gel. To maintain the proper parallelism between the slide and the cover-slip, two sacrificial, short pieces of SMF-28 are used as spacers. The length of the fiber used in a typical writing experiment is two meters with a central portion being in the assembly just described, and the rest hanging off either side. The total length of the fiber is chosen to ease the process of connectorizing the two ends with the diagnostic tools adopted to monitor the formation of the Bragg effect in real time. The sample so constructed, is then laid on the custom holder that has a cut-out designed to accommodate specifically a standard microscope slide.

The hanging portions of the fiber are held in tension by the magnetic clamps. This last step is critical for successful FBG writing. Tensioning the two ends of the fiber straighten its direction, easing the subsequent alignment, but also ensures that during fabrication, the fiber remains exactly in position during the writing process. At this point, because of the viscosity of the index-matching gel, the whole assembly is let to stand for about ten minutes, prior to laser processing.

At this point, the fiber needs to be aligned. First, the main axis of the fiber (defined as the x axis in figures 2 and 3) is set parallel to the motion direction of one of the two XMS stages. Once the fiber is locked into place with the magnetic clamps, it is already quite parallel to one of the main axes. All that is left to do are minor adjustments of the rotational axis of the M-37 stage which brings the fiber in perfect alignment. Second, the fiber core needs to be in the same z location for a total distance of at least 2 inches (50.8 mm). A small change in the z plane (≤ 1µm) during grating fabrication results in significant modifications in the intensity and structure of both the reflective and transmissive spectra of the FBG. Thus, an iterative process is employed to make sure that no z deviations are present along the fiber main axis. Specifically, near the starting x location, the fiber core is brought into focus adjusting the tip control of the M-37 stage. Then, the fiber is moved along the x direction for a distance of approximately 2 inches (50.8 mm) and the core is brought into focus by adjusting the microscope objective fine position. These two steps are repeated iteratively until the fiber core remains in perfect focus along the entire 2-inch (50.8 mm) length of the section of fiber to be processed..

It is obvious that this alignment procedure can only be as good as the quality of the manual and computer-controlled motion hardware employed in the *femtoFBG*, as well as its imaging system. For what concerns the motion part, the femtoFBG uses Newport high-performance stages, leading to a system that provides high sensitivity and outstanding trajectory accuracy in a compact, robust, and cost effective package. Figure 5 shows three images of SMF-28 fiber in the index-matching gel. These different imaging plane images were recorded after the alignment procedure. In two images the core is ±5 µm out of focus, while in one image the core is in focus. These images show clearly how capable the *femtoFBG* imaging system is in discerning the boundaries between the fiber core and cladding. Moreover, they show how the core/cladding boundaries almost disappear when the core is brought into focus. Since this effect is strongly dependent on the z position, it is used by the operator to perform the tilt adjustments required to bring the fiber in perfect alignment with the system axes.

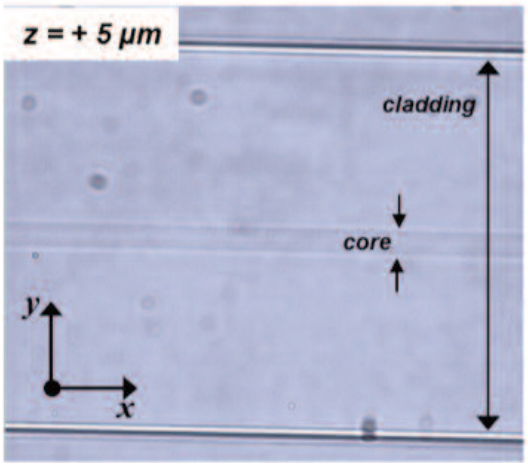

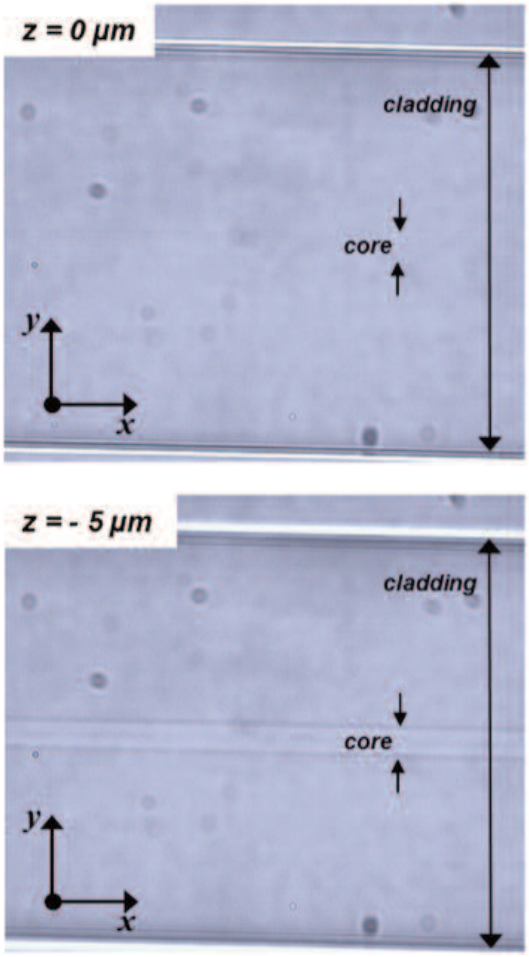

Figure 3 – *Pictures of an SMF-28 fiber assembly (see text for details) recorded using the femtoFBG imaging system. The imaging plane is defined by the x and y axes with the length of the fiber in the x direction. While the fiber core and cladding can easily be differentiated by a z position slightly off focus (± 5 µm), the boundaries between the glass zones blur into an undifferentiated image at the focal plane. These series of images demonstrate the excellent imaging capability of the femtoFBG, which is required for proper sample alignment. The width of the fiber cladding is 125 µm, while the width of the fiber core is 9.3 µm.*

femtoFBG– Examples

Transmission and reflection spectra of a PbP FBG fabricated with the *femtoFBG* are shown in Figure 6(a). Femtosecond laser direct-writing was carried out with a Spectra-Physics Spirit laser using its visible output at 520 nm. The tunable laser repetition rate was set at 200 kHz. Furthermore, the train of laser pulses reaching the fiber core was reduced to a rate of 63 Hz by means of the laser internal pulse picker. After aligning the sample and after setting the laser energy per pulse to 500 nJ, the fiber was translated along its main axis at a constant velocity of 100 µm/s for a total distance of 10 mm. Each laser pulse produced a grating plane, and the distance between adjacent laser-induced planes was 1.6 µm (Figure 6(b)). Therefore, the optical characteristics of the modified fiber shown in Figure 6 are a

shown in Figure 6 are a consequence of the fabrication of a 3rd order FBG operating at 1560 nm (eq. 1). The fabrication of this FBG took a total of one and a half minutes to be completed. Manufacturing time of PbP FBG can be shortened to few seconds using the proper combination of laser repetition rate and stage translational velocity (eq. 4).

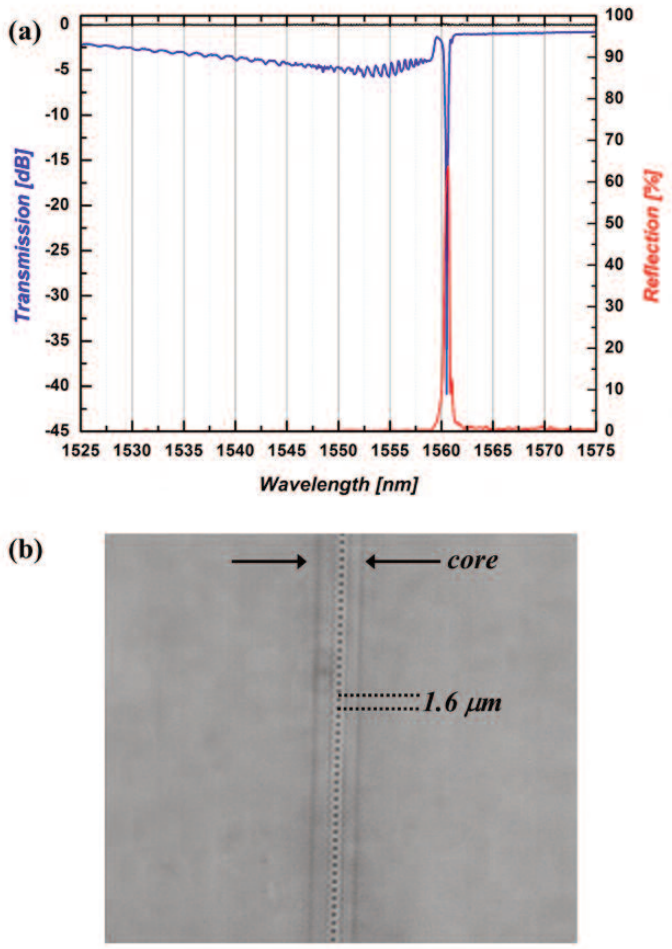

Figure 6 – *Transmission (blue) and reflection (red) spectra (a) of an FBG manufactured with the femtoFBG using the PbP writing method where each point was created with a single laser pulse. The reference spectrum (transmission of the probing light through the unadulterated fiber) is shown in black. An image of the written FBG, recorded by transmission light microscopy, is shown in (b).*

The transmission spectrum of the FBG in Figure 6 shows an impressive band rejection, with a strength reaching almost -40 dB which equates to a transmission of only 0.01%. The corresponding reflection spectrum is 65%. The linewidth of the grating resonance is less than 0.5 nm wide in both transmission and reflection spectra. The optical characteristics of the FBG shown in Figure 6 are excellent, enabling effective employment in several applications ranging from fiber lasers to sensing devices.

The asymmetry in the intensities of the transmission and reflection spectra shown in Figure 6 is a feature found commonly in femtosecond laser written FBGs. Theoretically, the amount of light rejected in transmission should be all reflected backward by the Bragg grating. In practice, this does not occur because of two mechanisms within the written fiber that cause optical losses. One of the mechanisms is light scattering which, in the case of the FBG in Figure 6, is less than -2 dB. This number comes from the drop in the intensity of the transmission spectrum observed for wavelengths longer than λ_{FBG} (i.e. insertion loss). The other mechanism is a significant coupling to cladding modes which is observed only in the transmission spectra. Furthermore, it covers a broad spectral window at wavelengths shorter than λ_{FBG}. A simple experiment can be performed to demonstrate the nature of the coupling between a guided mode core and the cladding modes in an FBG. First, the *femtoFBG* is used to fabricate an FBG in SMF-28. The writing conditions are similar to the ones used in the previous example with the exception of the grating period. Next, the fiber is stripped of its polymer coating. Finally, the optical transmission of the FBG is measured under two different environments. In one case, the fiber is left in air, while in the other case the fiber is completely immersed in index-matching oil. The resulting transmission spectra are shown in Figure 7. While a strong and sharp Bragg wavelength is observed at 1582 nm in both spectra, the profiles differ greatly for wavelengths shorter than λ_{FBG}. When the stripped fiber is immersed in index matching oil (Figure 7(a)), it simulates an infinite cladding. In this case, a smooth and declining transmission is displayed which is caused by radiation-mode coupling. Because the refractive index of the oil is not a perfect match with the cladding refractive index, small beating patterns are still observed. When the medium surrounding the fiber is air (Figure 7(b)), coupling to specific cladding modes is enhanced, resulting in clear and strong resonance dips.

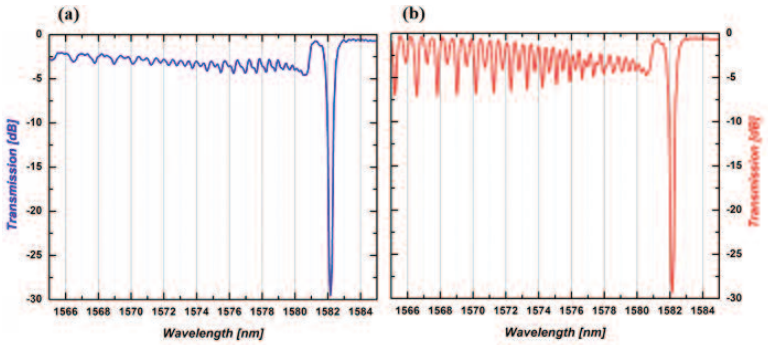

Figure 7 –*Transmission spectra of an FBG manufactured with the femtoFBG. The fiber was stripped of its polymer coating. In (a) the fiber was immersed in index-matching oil, while in (b) it was surrounded by air.*

PbP FBG manufacturing can be performed also using bursts of laser pulses instead of the more traditional single-shot, single-pulse method. In this approach, the fiber core is exposed to the laser beam in a stationary position for a predetermined amount of time. With the laser beam blocked, the fiber is then moved to a new position where laser irradiation will again occur.

The process is repeated along the fiber main axis as many times as necessary to cover the total length of the desired Bragg grating. Thus the femtoFBG is capable of offering the operator the flexibility to choose the number of laser pulses creating a single plane in the Bragg grating.

Transmission and reflection spectra of an FBG created with the *femtoFBG* following this procedure are displayed in Figure 8. The laser employed in the writing of the FBG was a Spectra-Physics Spirit with emission wavelength and repetition rate of 520 nm and 200 kHz, respectively. Each plane of the grating was created in the core of unstripped SMF-28 with a burst of 50 laser pulses. The energy per pulse was set to 170 nJ. The grating was 7 mm long and the period chosen between the laser bursts was 1.6 µm. This time, fabrication took ten minutes to complete. The grating, so created, produced a strong Bragg wavelength at around 1560 nm. There are several affinities with the spectral properties of the PbP FBG shown in Figure 6 (a). In both cases, sharp peaks with less than 0.5 nm linewidths are produced at the resonance wavelengths. Strong rejection bands are observed also, with the energy not being completely reflected in a backward direction. Nonetheless, the transmission spectrum in Figure 8 exhibits a more pronounced coupling to cladding modes than the transmission spectrum in Figure 6(a). This is most probably caused by the difference in material change caused in the fiber core by the two irradiation regimes. The energy deposited in the fiber used in Figure 8 during the Bragg grating writing process is indeed larger than the energy deposited in the fiber used in Figure 6(a). Consequently, the alteration of refractive index and morphology of the irradiated areas must be different in the two writing methods, leading to different optical losses.

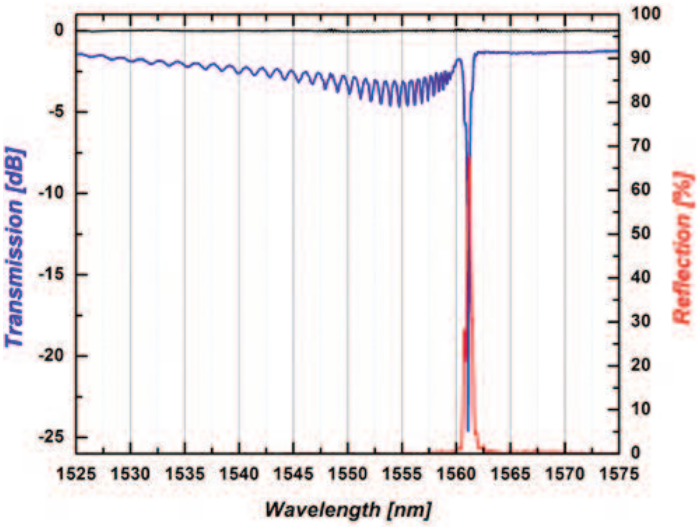

Figure 8 – *Transmission (blue) and reflection (red) spectra of an FBG manufactured with the femtoFBG using the PbP writing method where each point was created with a burst of 50 laser pulses. The reference spectrum (transmission of the probing light though the unadulterated fiber) is shown in black.*

An example of an LbL FBG fabricated with the *femtoFBG* is shown in Figure 9. The grating was written in the core of an unstripped SMF-28 fiber using the 520 nm output of a Spectra-Physics Spirit laser. The repetition rate and energy per pulse of the laser were set at 200 kHz and 150 nJ, respectively. A series of parallel lines 30 µm long were written across the fiber core (y direction in figure 3) separated by a distance of 1.64 µm (x direction in figure 3). The finished Bragg grating was 9 mm long and considering that fabrication was performed at a speed of 100 µm/s, the whole writing process took thirty minutes. The spectra in Figure 9 correspond to a 3rd order LbL FBG and it displays an impressive transmission attenuation of -36 dB with a full width at half maximum of 0.3 nm. Compared to the PbP FBG (figure 6), the LbL FBG exhibits a smaller insertion loss. This is most probably due to a more uniform change of refractive index in the laser processed areas of the fiber. Nonetheless, the LbL FBG still shows pronounced coupling to cladding modes at wavelengths smaller than λFBG.

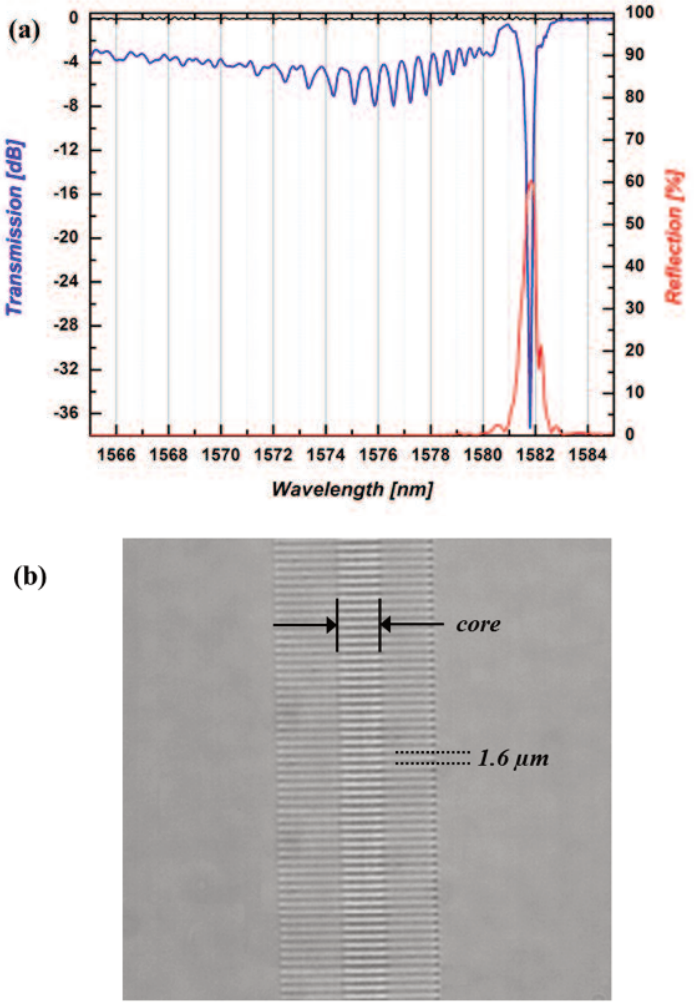

Figure 9 – *Transmission (blue) and reflection (red) spectra of an FBG manufactured with the femtoFBG using the LbL writing method (a). The reference spectrum (transmission of the probing light though the unadulterated fiber) is shown in black. An image of the written FBG, recorded by transmission light microscopy, is shown in (b).*

The *femtoFBG* is thus capable of creating high quality FBGs using both PbP and LbL methods. LbL writing might be considered a superior manufacturing method to PbP writing, since it allows the operator to adjust almost all the grating parameters. One has to remember though, that femtosecond laser direct-writing of FBGs is exceptionally sensitive to the alignment of the fiber core with the laser focal plane and with the direction of the motion of the stages. For example, errors must be contained within 1 µm for distances that can reach up to 10 mm. Thus, writing FBGs in the shortest amount of time possible is typically a good strategy for diminishing the detrimental effects of fluctuations in environmental conditions. In laboratories where temperature and humidity can vary rapidly then, PbP FBG writing is a better choice since it is more rapid than LbL FBG writing.

Conclusions and Future Vision

When used jointly with Spectra-Physics' Spirit laser, the femtoFBG becomes a remarkably flexible tool for femtosecond laser direct-writing of FBGs. It enables the operator to adjust (and hence tailor) FBG parameters such as central wavelength (λ_{FBG}) and its spectral width, strength of rejection band, and reflectivity. Furthermore, the *femtoFBG* is capable of writing FBGs by both PbP and LbL methods, with the freedom that only laser direct-writing can provide. Thus, the femtoFBG can be used to make apodized, chirped, sampled, tilted, and long-period Bragg gratings. Finally, the femtoFBG is not constrained to using only sensitized fibers, but is also capable of engraving refractive index changes in a variety of glasses independently of their level of dopants.

Although FBGs are already employed by several industries in a variety of applications, it is expected that their use in the near future will expand to other research areas where diagnostic tools are of the utmost importance. One such area is medical device manufacturing, where all sorts of chemical sensors are required in minimally invasive medical procedures. With the femtoFBG, we have developed a laser microfabrication tool that fits the needs of R&D laboratories where rapid, flexible, and consistent manufacturing of FBGs is required.

References

1. Hill K. O., Meltz G. J. *Lightwave Techn.* **15(8)**, 1263 (1997).
2. Mihailov S. J. *Sensors* **12**, 1898 (2012).
3. Kersey A. D., Davis M. A., Patrick H. J., LeBlanc M, Koo K. P., Askins C. G., Putnam M. A., Friebele E. J. *J. Lightwave Techn.* **15(8)**, 1442 (1997).
4. Dewra S., Vikas, Grover A. *Adv. Eng. Tec. Appl.* **4(2)**, 15 (2015).
5. Javanovic N., Fuerbach A., Marshall G. D., Ams M., Withford M. J. "Fibre grating inscription and applications" in Femtosecond Laser Micromachining, Osellame R. et al. eds, 197 (2012).
6. Othonos A. *Rev. Sci. Instrum.* **68(12)**, 4309 (1997).
7. Marshall G. D., Williams R. J., Jovanovic N., Steel M. J., Withford M. *J. Opt. Express* **18(19)**, 19844 (2010).
8. Lee B. *Opt. Fiber Techn.* **9**, 57 (2003).
9. Martinez A., Dubov M., Khrushchev, Bennion I. *Electr. Lett.* **40(19)**, 19 (2004).
10. Lai Y., Zhou K., Sugden K., Bennion I. *Opt. Express* **15(26)**, 18318 (2007).
11. Zhou K., Dubov M., Mou C., Zhang L., Mezentsev V. K., Bennion *IEEE Phot. Techn. Lett.* **22(16)**, 1190 (2010).
12. Martinez A., Dubov M., Khrushchev I., Bennion I. *IEEE Phot. Techn. Lett.***18(21)**, 2266 (2006).
13. Antipov S., Ams M., Williams R. J., Magi E., Withford M. J., Fuerbach A. *Opt.Express* **24(1)**, 30 (2016).
14. Gross S., Dubov M., Withford M. J. *Opt. Express* **23(6)**, 7767 (2015).
15. Nikogosyan D. N. *Meas. Sci. Technol.* **18**, R1 (2007).
16. Martinez A., Khrushchev I. Y., Bennion I. *Elect. Lett.* **41(4)**, 176 (2005).
17. Lai Y., Zhou K., Sugden K., Bennion I. *Opt. Express* **15(26)**, 18318 (2007).

mks | Newport™

www.newport.com | sales@newport.com
+1-949-863-3144 | +1-800-222-6440

DS-011701(09/19)